New miniature microstrip UWB antenna for biomedical wireless applications

YAQEEN S. MEZAAL[1,*], HIND S. GHAZI[2], ANSAM QASIM KAMIL[1], AQEEL A. AL-HILLALI[3], KADHUM AL-MAJDI[4]
[1]*Mobile Communication and Computing Engineering Department, University of Information Technology and Communications, Iraq*
[2]*Media Technology and Communication Engineering Department, University of Information Technology and Communications, Iraq*
[3]*Al-Farahidi University, Baghdad, Iraq*
[4]*Ashur University, Baghdad, Iraq*

This paper presents the design, simulation and fabrication of a new microstrip antenna belonging to the Ultra-Wideband (UWB) category, operating in the frequency range of 3.8973 GHz to 11.251 GHz. The antenna design integrates a Coplanar Waveguide (CPW) feed line and a hexagonal slotted fan-shaped net resonator, employed on an FR4 substrate with a dielectric constant of 4.4 and thickness of 1.6 mm. From the outcomes of this research, it is clear that the antenna model can cover the entire UWB frequency range with an operational bandwidth of 7.3536 GHz and an input return loss lower than -10 dB and unlike conventional planar antennas or microstrip patch antennas; this antenna has bipolar radiation patterns. Given its low weight, favorable radiation pattern as well as frequency response, the compactness of this antenna creates it a suitable candidate for potential medical applications in WBANs and healthcare applications. Accordingly, it can be one of the most promising technology alternatives targeting wireless communication and sensing in next-generation healthcare solutions.

(Received February 8, 2024; accepted August 1, 2024)

Keywords: UWB, FR4 substrate, Bi-polar radiation patterns, Compactness, Healthcare monitoring

1. Introduction

The traits of Ultra-wideband (UWB) technology include fast data transmission speeds, low electricity usage and minimal disruption making it popular in diverse biological applications. In UWB systems, microstrip antennas especially with CPW feeds or monopole have the role of transmitting and receiving signals due to their small size, ability to integrate and high performance [1-4]. There is an increasing need for small-sized antenna able to work within diverse frequency ranges especially when used for Medical Implant Communication as communication system devices become smaller. Microstrip antennas are suitable for UWB applications because they are planar in geometry, light weight and can operate at higher frequencies. The existence of the 3.1-10.6 GHz frequency band or its varieties has propelled research into UWB technology for imaging radar, remote sensing and localization and short-range wireless communications purposes as well. Printed monopole antennas on substrates offer wide impedance bandwidths compatible with UWB frequencies explored using different shapes such as rectangular, circular disc, ellipse and binomial curve design among others. It is important to test antennas used for UWB, Bluetooth, WLAN and other applications in different media within the ISM band in order to enable practical implementation [5-11].

Antennas are crucial for wireless capsule endoscopy (WCE) and healthcare, which enables imaging of the human intestines. Nonetheless, very short pulse durations creating an obstacle to attain exact receptor time synchronization through UWB. This technology's use in Wireless Telemetry Service for Health Care (WMTS and ISM) indicates its potential impact on health care applications. The 2.484 GHz ISM band is commonly employed for such applications as Bluetooth or WLAN. Therefore, it is necessary to test antennas under different conditions in order to carry out real-life projects. For instance, WCE systems depend on 433 MHz ISM band antennas in taking images of the intestines of humans. However, the main challenge with achieving precise receptor time synchronization using ultra-short pulse times lies within this aspect of medical methodologies that utilize UWB [12-20]. The study in [21] emphasizes on the relationship between UWB technology and antenna design for biomedical applications. These bands of UWB have large frequency spectrum which makes them ideal for biomedical applications in medicine, security, drug detection among others. Antennas with increased gain and directivity vibrate efficiently at higher frequencies, thus supporting activities like cancer detection, healthcare monitoring in real time as well as distance monitoring. In this case, biomedical microwave imaging systems can employ slot elements under UWB bands for compact

antennas such as corrugate tapered slot antenna (CTSA) to support wireless body area networks compliant to the IEEE 802.15 standard [22]. Antennas designed for UWB systems that operate perfectly from 3 to 10.6 GHz offer hope for IR-UWB operations within the range of 3.1-10.6 GHz due its good performance even within the IR-UWB bandwidth of 640 MHz to 7.2 GHz [20-23]. The low electromagnetic radiation of UWB systems, below -41.3 dBm/MHz, ensures safety for human tissue exposure, making them suitable for home and hospital applications [23]. Notably, this article outlines the process of creating miniature microstrip UWB antennas tailored for biomedical use, emphasizing their potential significance in microwave imaging. The reported article in [24], concentrates on developing a battery-free smart-textile-based energy harvester to power IoT-enabled wearable sensors, particularly in e-healthcare applications. This harvester, digitally embroidered and straightforwardly integrated into clothing, uses a multiport design to harvest energy from various directions and power sensors. With a simplified and miniaturized design, the harvester produces a beam with peak gain and wide beam width. Simulations and experiments validated its performance, and integration into IoT sensor nodes demonstrated real-time data collection without external batteries. Smart textiles and energy-harvesting technology offer self-sustaining solutions for wearable devices, improving functionality, predominantly in e-healthcare.

In the current study, the proposed microstrip antenna with UWB characteristics in the frequency range of 3.8973 GHz to 11.251 GHz holds significant potential for various medical applications. The proposed UWB microstrip antenna presents a promising solution for medical applications like remote patient monitoring systems, wearable health monitoring devices, and medical imaging technologies that rely on WBANs. It has highly compact size, highly wide bandwidth, and favorable radiation patterns as compared with many testified antennas in literature. These features make it an attractive choice for enhancing connectivity and data transmission in healthcare settings. The manuscript is organized as follows: The second section presents the design methodology of the proposed CPW-UWB antenna, including the antenna geometry, design parameters, and simulation setup. The third section discusses the consequences of the antenna's performance, including S11 response, radiation patterns, gain characteristics, etc. The fourth section provides a comparison between simulated and measured results to validate the proposed design. Finally, the last section concludes the paper and discusses potential future work for further improvements in the antenna design.

2. Design of UWB Antenna

The topology of the microstrip UWB antenna is indeed based on the coplanar waveguide (CPW) technology, which is well-suited for high-frequency applications in wireless communication systems, radar systems, and satellite communication. The use of coplanar waveguides offers advantages such as low loss, compactness, ease of integration with other components, and wide bandwidth, making them ideal for UWB antenna designs [25-30].

In the specific case of the hexagonal slotted fan-shaped topology used in the antenna design, several design choices and dimension parameters were considered to achieve the desired UWB characteristics as depicted in Fig. 1 and Table 1. The selection of the substrate dimensions, such as 25 mm × 27 mm × 1.6 mm, plays a crucial role in determining the operating frequency range and performance of the antenna. These dimensions are optimized by CST simulator to resonate within the UWB frequency band ranged from 3.8973 to 11.251 GHz, ensuring that the antenna can efficiently transmit and receive signals across this wide frequency range.

Using a 50-ohm microstrip line coupled to a coaxial cable for powering the radiator is a common configuration in antenna designs, providing a balanced impedance match for efficient signal transmission. The presence of the CPW feeder, ground plane, and dielectric substrate in the same plane simplifies the antenna structure and allows for compact and cost-effective production.

Table 1. The dimensional parameters of CPW- UWB Antenna

Parameters	Dimension in (mm)	Parameters	Dimension in (mm)	Parameters	Dimension in (mm)	Parameters	Dimension in (mm)
W s	25	P1	3	P6	2	P11	2
Ls	27	P2	8	P7	1	P12	6
W_f	3	P3	6	P8	1	P13	4
L_f	12	P4	4	P9	1	P14	11
W_1	1	P5	3	P10	1	P15	10

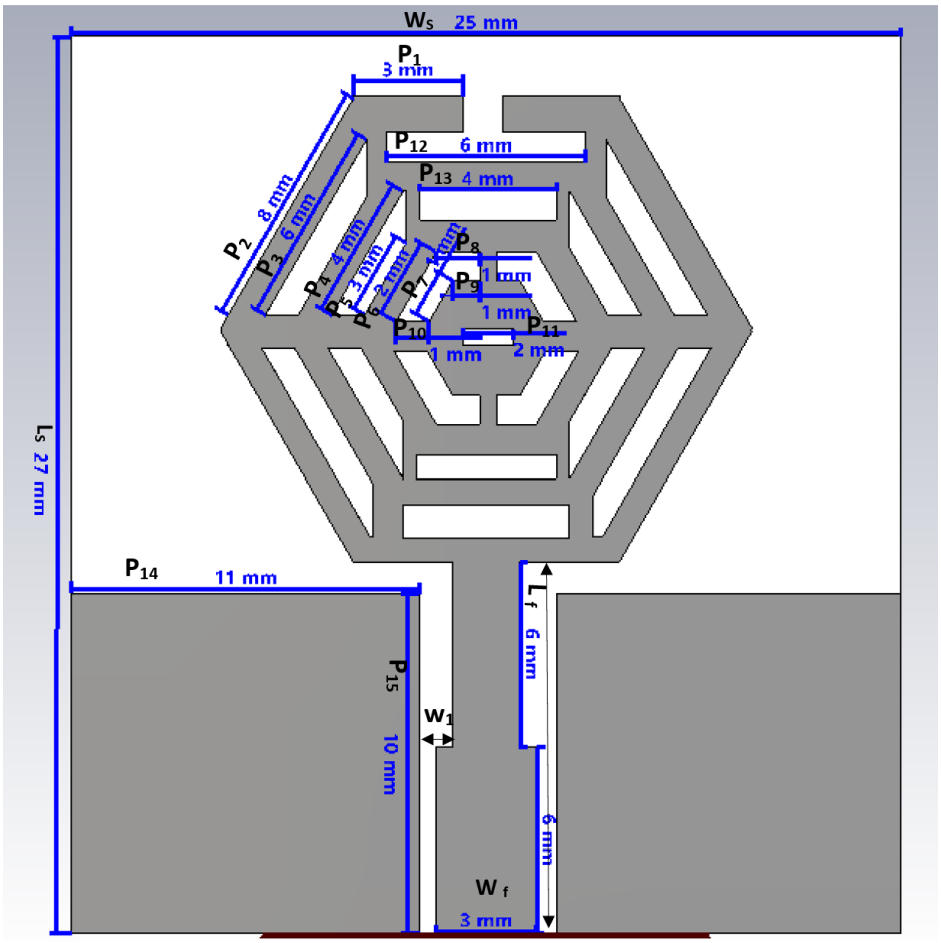

Fig. 1. Antenna structural design and dimensions

Fig. 2 shows the input reflection response of RLC equivalent circuit for the projected UWB antenna as generated by the microwave office simulator. Capacitors and resistors are connected in parallel. Varying the values of the resistors and capacitors can be employed to modify the input reflection of an antenna circuit. Using the first and last inductors can be adopted for changing impedance bandwidth range. The study's predicted antenna ranges are so close to the impedance bandwidths of ultra wide band (UWB) that it is expected to be 3.4 GHz – 11.349 GHz. CPW-UWB antenna designs which will employ RLC tank circuits should be used for achieving very broad bands. For this reason, the RLC tank circuit is composed of an inductor (L), a resistor (R), and a capacitor (C), connected in parallel or series and it can be tuned to different frequencies thereby enhancing the antennae performance across a wide frequency band. When selecting an RLC tank circuit configuration for CPW-UWB antennas, designers must take into account issues such as desired bandwidths, radiation efficiency and required parameters for impedance matching. By carefully choosing component values within the RLC tank circuit, designers can manipulate antenna resonances at multiple points throughout UWB spectra, which allows efficient data transmission/reception. However, with respect to using RLC tank circuits on CPW-UWB antennas, one must weigh against increased complexity in tuning/optimizing them for operation over wider bands. Designers may have to change their component values many times before they get the necessary performance from these devices leading to wastage of time and energy during this exercise. In contrast, alternative approaches such as using lumped elements or distributed components in the antenna design may offer simpler tuning processes, but may not provide the same level of flexibility and control over the antenna's wideband characteristics.

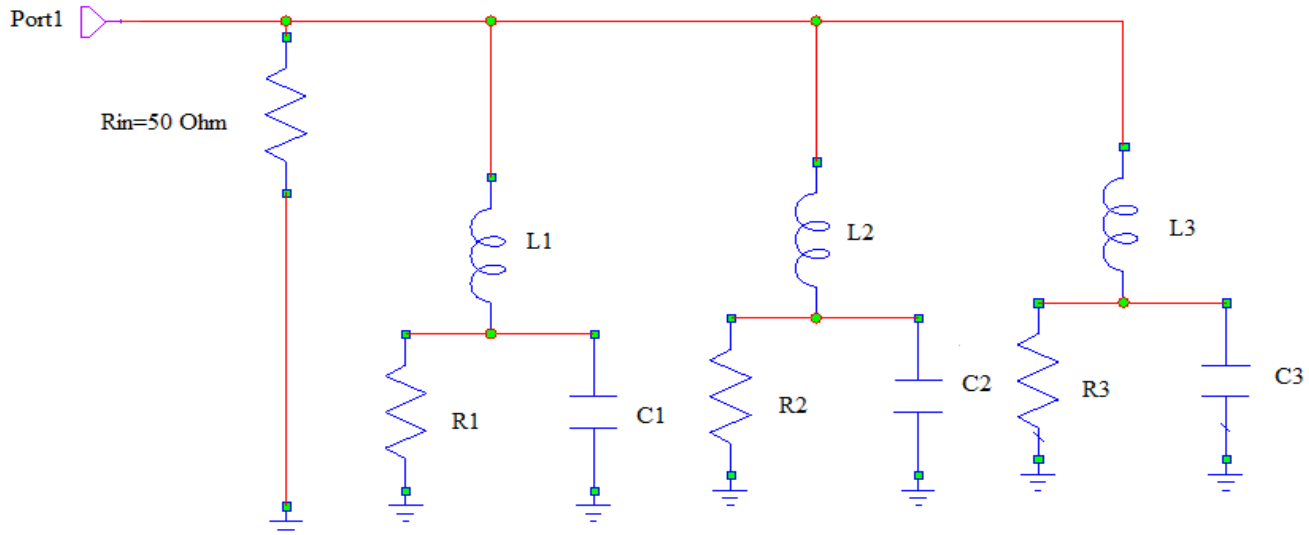

(a)

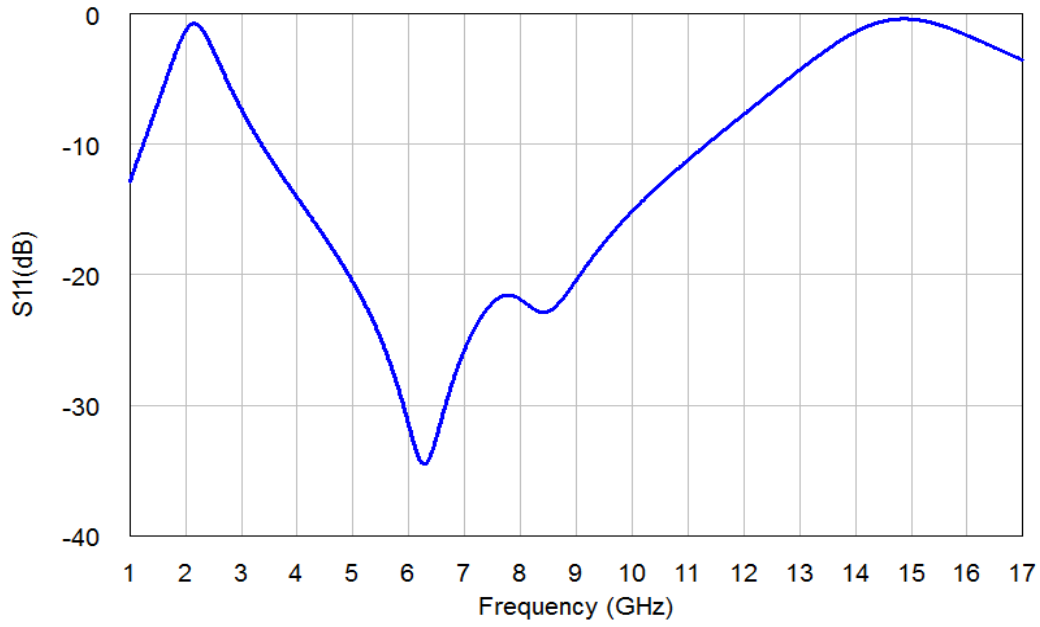

(b)

Fig. 2. (a) The equivalent RLC circuit for the proposed antenna and (b) its S11 result. L1=5 nH, L2=40 nH, L3=1.15 nH, R1=2000 Ω, R2=10000 Ω, R3=10000 Ω, C1=1.1 pF, C2=0.01 pF, C3=0.1 pF

3. Simulation results

The designed microstrip CPW-UWB antenna is simulated by CST Microwave Studio software. The simulation consequences show that the antenna has a wideband response with a bandwidth of 7.3536 GHz (3.8973 GHz to 11.251 GHz). In general, CST simulator analyses 3D and multilayer architectures. It has been widely employed in the design of many antenna designs. It can compute and depict the return loss, standing wave ratio from Smith charts, real power vs frequency, VSWR, E-field and H-field distribution, gain, and radiation patterns. This feasibility produced good results with impedance bandwidth of 7.3536 GHz and a center frequency of 7.57 GHz. Return loss can be considered as basic way to typify the input and output of signal sources, or when the load is mismatched or when not all of the existing produced power is given to the load. The projected antenna's S11 parameter has been evaluated, and the simulated consequence for S11 response is depicted in Fig. 3. The return loss was reached to -18dB, which is feasible theoretically.

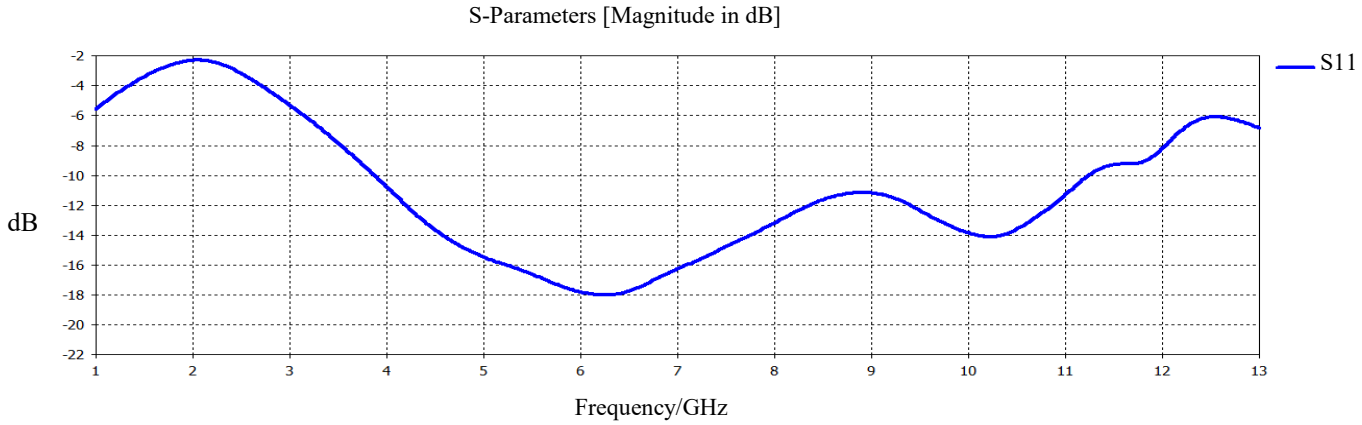

Fig. 3. Input reflection (S11) response for proposed UWB antenna

The surface current distribution in the areas for the considered UWB antenna at 3 GHz is illustrated in Fig. 4. At 3 GHz, the maximum magnetic strength was 101 A/m, and the effectual areas have been noted in the feeder, at the patch radiator's base.

At a frequency of 7 GHz, the projected UWB antenna exhibits 3D radiation patterns as depicted in Fig. 5, with a maximum gain of 2.7 dBi.

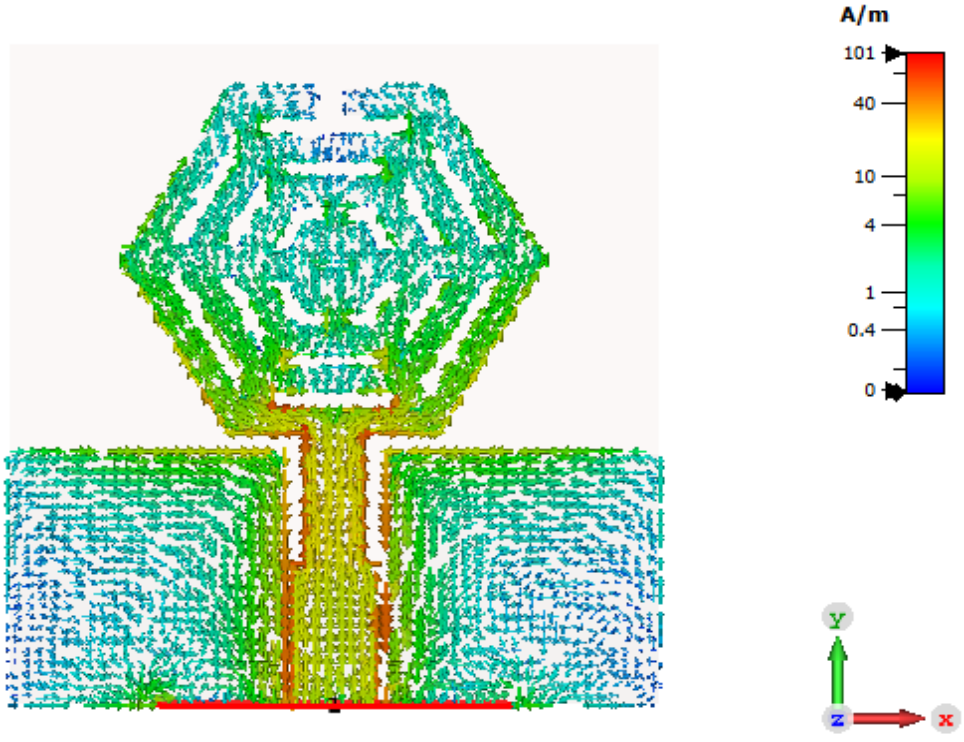

Fig. 4. Surface current intensity distribution of the antenna at 3GHz (color online)

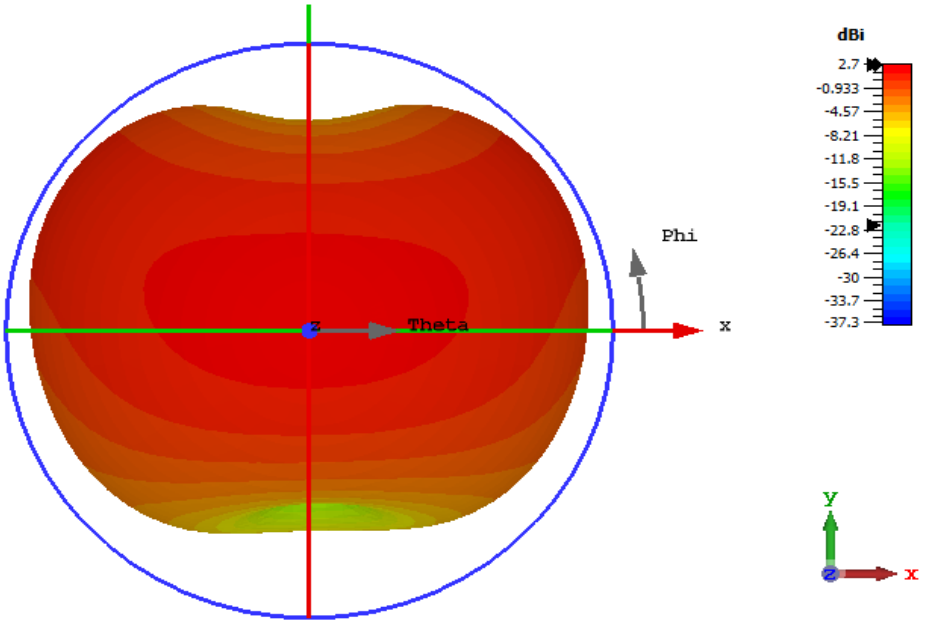

Fig. 5. 3D radiation patterns of the proposed UWB antenna (color online)

Fig. 6 illustrates the UWB gain values within UWB frequency range of the proposed UWB antenna with peak gain of 4.725 dBi. It is important to note that there is a direct proportionality between the antenna gain and the square of the operating frequency. This relationship is depicted in Fig. 6, while efficiency remains unaffected by this correlation. The primary factors leading to a decrease in efficiency include conduction loss, dielectric loss, and slightly restricted feedline-antenna impedance matching.

An important aspect of antenna design is the consideration of losses, which can impact various factors. When the size of the antenna is comparable to or larger than the wavelength, a reduction in directivity occurs, resulting in the appearance of side lobes. The antenna exhibits a bi-polar radiation pattern, as shown in Fig. 7. This pattern indicates that the antenna emits or collects electromagnetic energy in two opposite directions, resulting in two significant lobes of radiation strength on either side of the antenna structure.

The bi-polar radiation pattern allows for symmetrical radiation around the antenna axis, with energy broadcasted in two opposing angles with uniform strength. This pattern is commonly observed in antennas designed for symmetrical radiation in two directions, featuring two main peaks in the radiation pattern oriented differently based on the antenna design.

The offset beam pattern generated by the bi-polar radiation pattern enables signal coverage in multiple directions, akin to transpiration systems. The radiation pattern at different frequencies demonstrates symmetrical behaviors, ensuring consistent performance. Assessing antenna performance involves comparing the total power received from the generator to the total radiated power by the antenna. Optimal radiation extends into the surrounding empty space, while inefficient radiation results in energy losses due to factors like magnetic, dielectric, and metal conduction losses.

Fig. 8 displays the radiation efficiency of the designed antenna, with minimum efficiency at 1.5 GHz (6.7%) increasing significantly, as frequency rises, reaching 92% at 6.43 GHz. Table 2 compares the proposed CPW- UWB antenna with existing antennas in the state of the art, highlighting its compact dimensions and extensive impedance bandwidth.

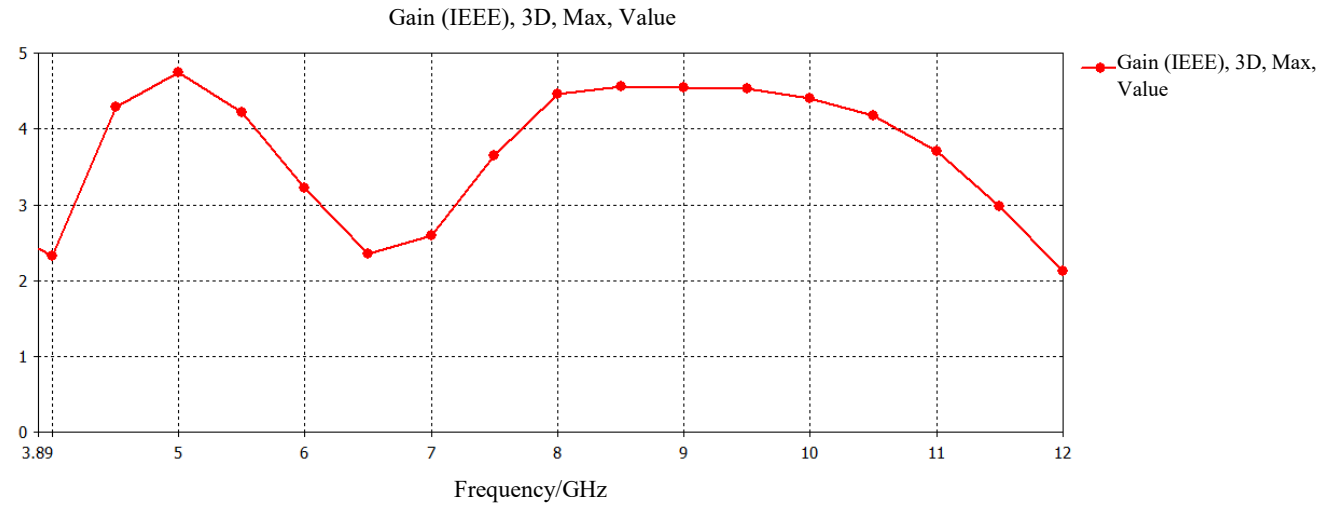

Fig. 6. Gain for designed CPW-UWB antenna

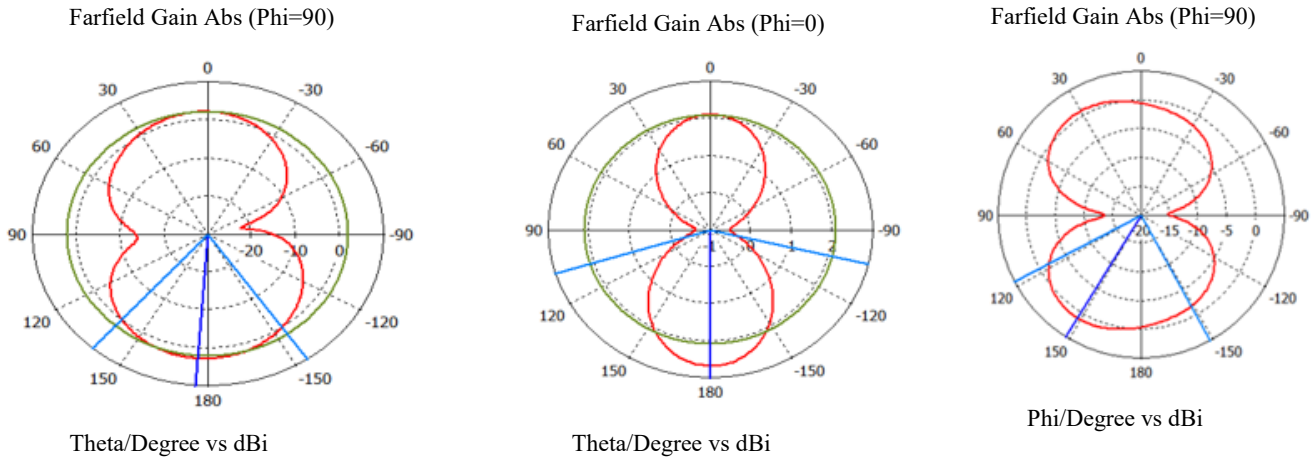

Fig. 7. Radiation patterns for designed CPW-UWB antenna at 7 GHz (color online)

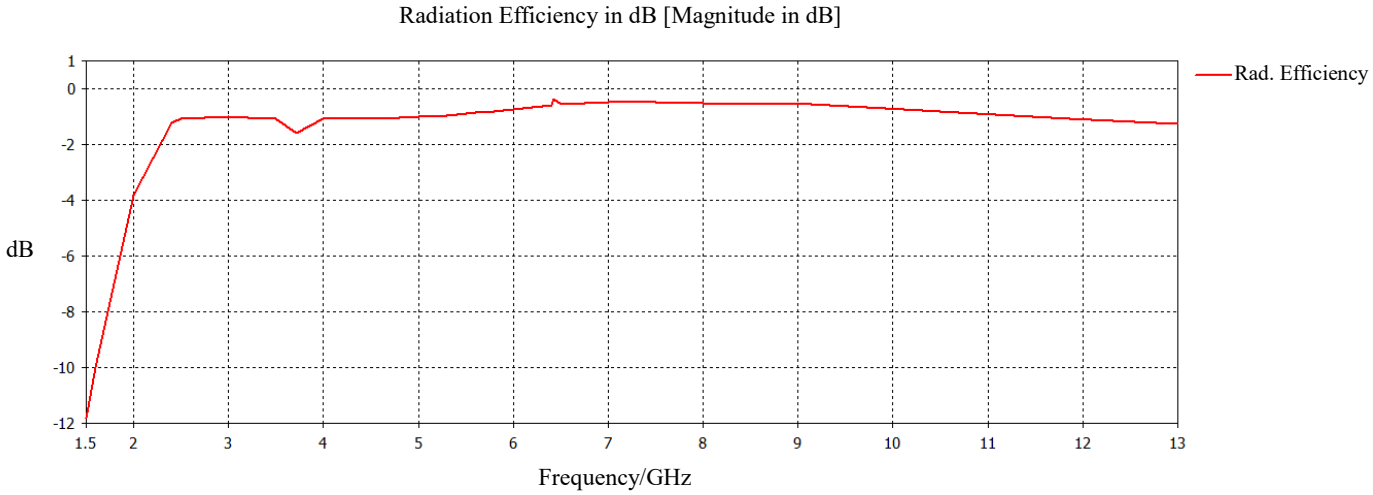

Fig. 8. Radiation efficiency for the CPW-UWB antenna (color online)

Table 2. Comparison of our proposed antenna with other ones in literature

Ref.	Dielectric Constant	Size (mm^2)	Bandwidth Range (GHz)	Applications
This work	4.4	25× 27	3.8973-11.251	WBANs and healthcare
[31]	3.16	40 × 38	2-12	Near-field microwave imaging
[32]	4.4	26 × 29	3.1–10.6	Near-field microwave imaging
[33]	10.2	19 × 19	2-8	Near-field microwave imaging
[34]	10.2	25 × 36	1-9	Near-field microwave imaging
[35]	10.2	50 × 50	1-9	Near-field microwave imaging
[36]	1.15–1.3	70.3 × 37	3-10	Microwave imaging systems
[37]	9	62.5 × 62.5	2–4.4	Microwave imaging systems

The designed antenna in the paper may generate multiple modes due to its complex geometry and operating frequency range. The primary mode of operation for the microstrip antenna design is likely to be the fundamental resonant mode of the patch structure. This mode is typically responsible for the main radiation characteristics of the antenna. The coplanar waveguide (CPW) feed line used in the antenna design may also generate its own modes, especially at higher frequencies. These modes can affect the impedance matching and overall performance of the antenna. Due to the complex geometry of the hexagonal slotted fan-shaped net, the antenna may support higher order resonant modes that contribute to the overall bandwidth and radiation characteristics of the antenna. The FR4 substrate with a dielectric constant of 4.4 and thickness of 1.6 mm can also support substrate modes, which can interact with the antenna structure and affect its performance. The bi-polar radiation patterns mentioned in the paper suggest that the antenna may support dual-polarization modes, which can provide diversity and flexibility in signal reception and transmission.

4. Fabrication and measurement

The microstrip CPW-UWB antenna is fabricated on a FR4 substrate with a thickness of 1.6 mm as in shown prototype in Fig. 9. The dimensions of the patch and ground plane are optimized based on the simulation results. The antenna is connected to a coaxial cable and S11 readings are taken by a vector network analyzer (VNA).

Several reasons may account for allowable differences between the simulated and measured S11 responses indicated in Fig. 10 for a fabricated CPW-UWB antenna. In spite of targeting high precision during antenna fabrication, tiny tolerances may still result from deviations in manufacturing dimensions of the antenna elements. Such small inaccuracies can affect the performance of an antenna leading to deviation between the measured S11 response and simulated results. Besides, this may also be influenced by variations in dielectric properties on FR-4 substrate as resulted from manufacturing processes that deviate from calculated material parameters thus affecting such an antenna's performance too. Changes in dielectric constant or loss tangent could cause disparities between simulated and measure S11 responses. Unaccounted reflections by connector effects during measurement can modify S11 values, which are not taken into consideration during simulation. This leads to discrepancies between actual measurement and simulated results. Environmental elements such as electromagnetic interference or objects nearby when measurements are done can introduce errors resulting into distortion of the S11 response.

These external forces are usually left out in simulations and can cause difference between simulated and real results. Errors of calibration on vector network analyzer measurements could bring about uncertainties that affect the accuracy of the measured S11 response. However, even minor departures from calibration will lead to a discrepancy with respect to the simulative responses. The assumptions made during simulation in commercial microwave antenna design models may involve some simplifications or idealizations which do not exactly show what happens in real life. For certain scenarios where there is complexity or non-ideal behavior, these assumptions will cause mismatches between simulations and measured performance.

At any rate, the measured impedance bandwidth is ranging from 3.6 to 11.8 GHz (bandwidth value = 8.2 GHz) compared to the simulated one (7.3537 GHz). Therefore, almost 11.5% error or deviation between the measured impedance bandwidth and the simulated impedance bandwidth has been reached so far. This shows that measurement of this bandwidth is quite near to its simulation counterpart with an acceptable level of agreement. These findings are agreed with measured S11 results in reported papers in [25-30].

Fig. 9. Fabricated prototype of the projected antenna

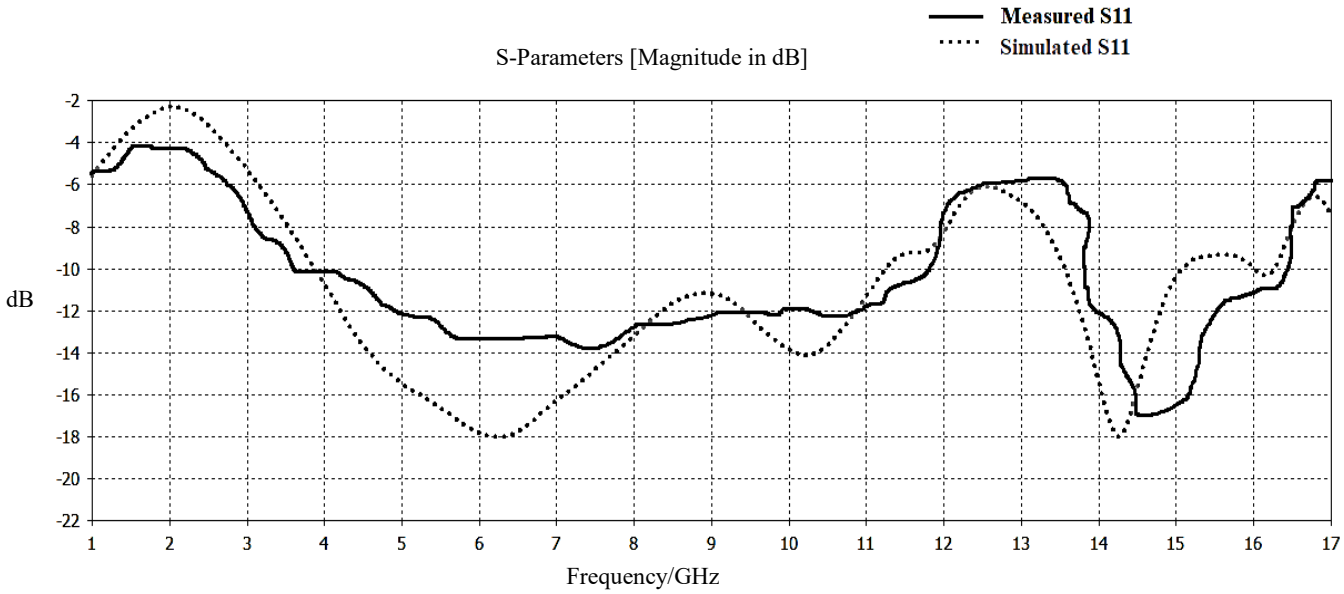

Fig. 10. Measured and simulated input reflection responses for the projected antenna

5. Conclusion

In conclusion, it is observed that the UWB microstrip antenna designed with CPW feed line and hexagonal slotted fan-shaped topology on FR-4 substrate has shown excellent performance for a wide frequency band spanning from 3.8973 GHz to 11.251 GHz with peak gain of 4.725 dBi. The proposed antenna therefore presents several advantages including its compactness, lightness, bipolar radiation patterns and tolerable frequency response which make it suitable for various medical applications including WBANs and medical imaging.

Its ability to transverse the entire UWB frequency range caters for reliable communication within healthcare settings. It exemplifies how well this antenna can enable innovative healthcare advancements. By integrating globally accepted communication standards, this antenna could even contribute significantly towards providing wireless connectivity among medical devices and assist hearing impaired patients.

While we are looking ahead, gain and radiation patterns can be, as future work, measured to validate the simulated ones. The future could be revolutionized by promising developments and deployments of advanced antenna technologies in healthcare delivery to better patient outcomes. Thus, this antenna design can be used by researchers and practitioners to create new areas for medical monitoring, diagnostics and treatment through continuously connected wireless communication systems. In reality, this work transcends the bounds of usual antenna designs that are found in many other sectors as it has the potential to transform healthcare industry and more.

References

[1] A. R. Azeez, S. A. Ahmed, Z. A. Abdul Hassain, A. A. Al-behadili, H. S. Ghazi, Y. S. Mezaal, A. A. Hashim, A. A. Al-Hilali, K. Al-Majdi, Journal of Mechanics of Continua and Mathematical Sciences, **19**(3), 40 (2024).

[2] N. Sharma, S. S. Bhatia, V. Sharma, J. S. Sivia, Wireless Personal Communications **111**(3), 1977 (2020).

[3] N. Sharma, S. S. Bhatia, International Journal of RF and Microwave Computer-Aided Engineering **31**(1), art. no. e22488 (2021).

[4] N. Sharma, S. S. Bhatia, V. K. Banga, International Journal of Electronics **110**(8), 1516 (2023).

[5] A. Latif, "Design of a UWB Coplanar Fed Antenna and Circular Miniature Printed Antenna for Medical Applications," IntechOpen, 2020.

[6] D. Sarma, A. O. Asok, S. Dey, "Designing a Meanderline-Based Ultraminiature Low-Profile Ultrawideband Antenna for Biomedical Applications," 2024 IEEE Wireless Antenna and Microwave Symposium (WAMS), 1 (2024).

[7] S. Modak, V. Kaim, T. Khan, B. K. Kanaujia, L. Matekovits, K. Rambabu, "Design and Performance Measurement of Worn-on-Body Instrumental Ultra-Miniaturized UWB Wearable Patch for e-Health Monitoring," IEEE Access **12**, 25719 (2024).

[8] M. Dilruba Geyikoglu, Analog Integrated Circuits and Signal Processing **114**(3), 439 (2023).

[9] H. T. Sediq, J. Nourinia, C. Ghobadi, B. Mohammadi, Biomedical Signal Processing and Control **80**, 104363 (2023).

[10] A. Biswas, A. J. Islam, A. Al-Faruk, S. S. Alam, 2017 International Conference on Electrical, Computer

and Communication Engineering (ECCE), 181 (2017).
[11] R. Bhatoa, E. Sidhu, 2017 International conference on big data analytics and computational intelligence (ICBDAC) 289 (2017).
[12] M. S. Miah, C. Icheln, K. Haneda, K. Takizawa, "Antenna systems for wireless capsule endoscope: Design, analysis and experimental validation," arXiv Prepr. arXiv1804.01577, 2018.
[13] X. Lin, Y. Chen, Z. Gong, B.-C. Seet, L. Huang, Y. Lu, IEEE Trans. Antennas Propag. **68**(6), 4238 (2020).
[14] V. Singh, A. Nag, E. Sidhu, 2016 International Conference on Wireless Communications, Signal Processing and Networking (WiSPNET), 927 (2016).
[15] J. M. Chowdhury, M. A. Rahaman, 2019 5th International Conference on Advances in Electrical Engineering (ICAEE), 653 (2019).
[16] B. J. Mohammed, A. M. Abbosh, P. Sharpe, Int. J. RF Microw. Comput. Eng. **23**(1), 59 (2013).
[17] T. Dissanayake, K. P. Esselle, M. Yuce, 2009 3rd European Conference on Antennas and Propagation, 3523 (2009).
[18] X. Li, M. Jalilvand, Y. L. Sit, T. Zwick, IEEE Trans. Antennas Propag. **62**(4), 1808 (2014).
[19] W. Rhee, N. Xu, B. Zhou, Z. Wang, 2010 International Conference on Information and Communication Technology Convergence (ICTC), 35 (2010).
[20] S. K. Mishra, R. K. Gupta, A. Vaidya, J. Mukherjee, IEEE Antennas Wirel. Propag. Lett. **10**, 627 (2011).
[21] R. Dhayabarani, C. Anitha, J. A. John, P. Gomathi, B. Hebsiba, 2018 Second International Conference on Inventive Communication and Computational Technologies (ICICCT), 1201 (2018).
[22] N. Chahat, M. Zhadobov, R. Sauleau, K. Ito, IEEE Trans. Antennas Propag. **59**(4), 1123 (2011).
[23] V. Cruz, J. N. Matos, P. Pinho, M. P. M. Pato, 2018 IEEE International Symposium on Antennas and Propagation & USNC/URSI National Radio Science Meeting, 1619 (2018).
[24] M. Zada, U. R. Iman, A. Basir, H. Yoo, IEEE Transactions on Industrial Electronics **71**(8), 9865 (2024).
[25] M. S. Jameel, Y. S. Mezaal, D. C. Atilla, Symmetry (Basel) **15**(3), 633 (2023).
[26] F. Abayaje, A. A. Alrawachy, Y. S. Mezaal, Optoelectron. Adv. Mat. **17**(7-8), 323 (2023).
[27] M. S. Jameel, Y. S. Mezaal, D. C. Atilla, Optoelectron. Adv. Mat. **17**(1-2), 78 (2023).
[28] Y. S. Mezaal, K. Al-Majdi, A. Al-Hilalli, A. A. Al-Azzawi, A. A. Almukhtar, Proceedings of the Estonian Academy of Sciences **71**(2), 194 (2022).
[29] D. O. Rodriguez-Duarte, J. A. T. Vasquez, R. Scapaticci, L. Crocco, F. Vipiana, IEEE Antennas Wireless Propag. Lett. **19**(12), 2057 (2020).
[30] M. Ojaroudi, S. Bila, M. Salimi, "A Novel Approach of Brain Tumor Detection using Miniaturized High-Fidelity UWB Slot Antenna Array," pp. 1-5, Mar. 2019 [Online]. Available: https://hal-unilim.archives-ouvertes.fr/hal-02377024.
[31] N. Tavassolian, S. Nikolaou, M. M. Tentzeris, Proceedings of the 2007 Asia-Pacific Microwave Conference, Bangkok, Thailand, pp. 1-4 (2007).
[32] T. S. See, Z. Chen, X. Qing, Proceedings of the 2009 Asia Pacific Microwave Conference, Singapore 2192 (2009).
[33] Y. Wang, A. E. Fathy, M. R. Mahfouz, Proceedings of the 2011 IEEE International Symposium on Antennas and Propagation (APSURSI), Spokane, WA, USA, pp. 2119-2122 (2011).
[34] X. Li, Jijing Yan, Malyhe Jalilvand, Thomas Zwick, Proceedings of the 2012 6th European Conference on Antennas and Propagation (EUCAP), Prague, Czech Republic 3677 (2012).
[35] X. Li, Y. L. Sit, L. Zwirello, T. Zwick, Microw. Opt. Technol. Lett. **55**, 105 (2013).
[36] C. H. See, R. A. Abd-Alhameed, S. W. J. Chung, D. Zhou, H. Al-Ahmad, P. S. Excell, IEEE Trans. Antennas Propag. **60**, 2526 (2012).
[37] X. Yun, E. C. Fear, R. H. Johnston, IEEE Trans. Antennas Propag. **53**, 2374 (2005).

*Corresponding author: Yaqeen.mezaal@uoitc.iq, yakeen_sbah@yahoo.com